ELSEVIER

Journal of Structural Geology 27 (2005) 447–457

JOURNAL OF STRUCTURAL GEOLOGY

www.elsevier.com/locate/jsg

Microstructural evolution during initial stages of static recovery and recrystallization: new insights from in-situ heating experiments combined with electron backscatter diffraction analysis

Michel Bestmann[a,*], Sandra Piazolo[a], Chris J. Spiers[b], David J. Prior[a]

[a]*Department of Earth Sciences, University of Liverpool, 4 Brownlow Street, Liverpool L69 3GP, UK*
[b]*Department of Earth Sciences, Utrecht University, Budapestlaan 4, 3584 CD Utrecht, The Netherlands*

Received 3 March 2004; received in revised form 25 September 2004; accepted 20 October 2004
Available online 28 January 2005

Abstract

We present in-situ observations, performed using electron backscatter diffraction, of static recovery and recrystallization processes occurring in a plastically deformed geological material, namely rocksalt. Static heating experiments, carried out in a scanning electron microscope at temperatures of up to 450 °C, allowed direct detailed observations of grain boundary migration between substructured grains in deformed polycrystalline samples. Contrary to expectations, crystallographic orientation maps reveal that behind slowly migrating grain boundaries new subgrain boundaries form while pre-existing subgrain boundaries are sometimes inherited. Moreover, the crystallographic character, especially the preferred orientation of misorientation axes of the new substructures reflects the character of the previous deformation history. These results imply that substructural features, such as subgrain misorientation distributions, may be relatively robust indicators of deformation mechanisms and conditions, even in tectonites that have undergone late, static recrystallization. In addition, our observations suggest that the process of static grain boundary migration does not necessarily reset earlier deformation microstructures as commonly assumed. The kinematic observations of boundary migrations are inconsistent with simple models in which migration is achieved by single atoms jumping across the boundary.

Keywords: Rocksalt; Microstructure; Grain boundary migration; Electron backscatter diffraction; In-situ heating

1. Introduction

The study and interpretation of microstructures developed in naturally deformed rocks, on the grain and subgrain scale, plays an important role in unravelling the history and dynamics of tectonic processes recorded in the Earth's crust (Means and Xia, 1981; Schmid, 1982; Hobbs, 1985). Recovery and recrystallization are two important processes that occur during or after tectonic deformation (White, 1977). Dynamic (syn-tectonic) recrystallization is indicated by the presence of deformed old and new grains showing irregular, i.e. sinusoidal boundaries and/or intracrystalline optical strain features, such as undulose extinction and subgrain boundaries. Static (post-tectonic) recovery and recrystallization, by comparison, is commonly assumed to be characterised by the presence of strain-free grains with straight or smoothly curved boundaries and a polygonal foam fabric. Interpreting natural tectonite microstructures, in terms of deformation processes and conditions, is largely based on comparisons with the final, frozen-in (post-mortem) microstructures observed in experimentally deformed rocks. Serial experiments in which the material is analysed before and after heating can provide a statistical analysis of microstructural changes during annealing, although direct correlation of individual grain boundaries or grains before and after heating is not possible (Heilbronner and Tullis, 2002; Barnhoorn, 2003). These analyses yield only limited information on dynamics of inter- and intracrystalline grain processes during

* Corresponding author. Current address: Department of Geological Sciences, University of Vienna, Althanstrasse 14/2B448, A-1090 Vienna, Austria
E-mail address: michel.bestmann@univie.ac.at (M. Bestmann).

0191-8141/$ - see front matter © 2005 Elsevier Ltd. All rights reserved.
doi:10.1016/j.jsg.2004.10.006

microstructural evolution. More useful data would come from real-time in-situ observations of microstructural evolution, under both static and dynamic conditions.

Until recently, only a few in-situ observations of grain boundary migration processes and substructural evolution have been carried out on polycrystalline minerals, i.e. nitratite (sodium nitrate), carnallite and bischofite, using optical microscopy (Tungatt and Humphreys, 1981; Urai, 1985, 1987; Drury and Urai, 1990; Urai and Jessell, 2001, and references therein). To obtain additional information on crystallographic orientation during microstructural evolution, in-situ experiments on rock analogue materials (e.g. octachloropropane, norcamphor, ice) were carried out using optical microscopy (e.g. Beck, 1949; Urai et al., 1980; Urai and Humphreys, 1981; Means, 1983; Wilson, 1985; Burg et al., 1986; Jessell, 1986; Means and Ree, 1988; Ree, 1990; Bons and Urai, 1992; Herwegh and Handy, 1996; Ree and Park, 1997; Zhang and Wilson, 1997; Nam et al., 1999; Park et al., 2001). During these experiments, analysis of the crystallographic orientations is limited to *c*-axis measurements. However, to characterise misorientation relationships across grains and subgrains, and the distribution of misorientation axes, the full crystallographic orientation needs to be known. The distribution of misorientation axes is a powerful tool to quantify microstructural features and to constrain deformation processes (e.g. Bestmann and Prior, 2003, and references therein). In-situ analyses in the transmission electron microscope (TEM) and in the scanning electron microscope (SEM), especially in combination with the electron backscatter diffraction (EBSD) technique, are able to provide the full crystallographic information needed and have already been applied for metals (e.g. Humphreys, 1979; Humphreys et al., 1996; Le Gall et al., 1999; Gemperlova et al., 2002; Seward et al., 2002, 2004). In addition, in-situ heating experiments, accompanied by automated crystallographic orientation mapping in the SEM (Humphreys, 2001; Seward et al., 2004), can be used to observe directly how microstructures change with time during static annealing or deformation. These data provide a sophisticated basis for interpreting the dynamics of inter- and intracrystalline processes of microstructural change (Piazolo et al., 2005b).

In the present study, we apply in-situ heating experiments, accompanied by automated crystallographic orientation mapping in the SEM to a geological material for the first time. At present it is not possible to perform in-situ heating experiments on major rock-forming minerals such as quartz and/or calcite. For example, in-situ heating experiments in the SEM have shown that calcite marble decomposes at $\sim$500 °C in the high vacuum chamber. Since no microstructural change occurred at $<$500 °C, no observations of such changes could be made (Bestmann, unpubl. data). Accordingly, we chose rocksalt for the following two reasons: (1) rocksalt is a useful silicate analogue material, since the grain and subgrain scale microstructures developed in deformed rocksalt at near ambient conditions are similar to those developed in silicate rocks at high pressures and temperatures (Guillopé and Poirier, 1979a; Drury and Urai, 1990); (2) the deformation behaviour of rocksalt plays an important role in controlling a variety of tectonic processes and hydrocarbon trapping phenomena (e.g. Duval et al., 1992; Jackson, 1995).

2. Materials and methods

2.1. Material and sample preparation

We conducted our study using samples of experimentally deformed, dry synthetic rocksalt. The rocksalt starting material was prepared by cold pressing and annealing analytical grade NaCl (Peach and Spiers, 1996). The resulting foam-microstructure was characterised by an average grain size of $\sim$350 μm and $\sim$60 ppm water content. Cylindrical samples of this material were dried in air for $\sim$24 h at 550 °C, reducing the water content to 2–5 ppm with negligible microstructural change (Trimby et al., 2000; Watanabe and Peach, 2002). These were then deformed in axi-symmetric compression in a triaxial deformation apparatus to 30% strain, at a strain rate of $\sim 6\times10^{-7}\,s^{-1}$ at 175 °C and a confining pressure of 50 MPa (Peach and Spiers, 1996). Samples of the deformed material were prepared for EBSD analysis from a cube of the deformed sample cut normal to the compression direction using a diamond wafering saw. This cube was further cut and ground, first into wafers and then into 'tiles' nominally measuring $9\times9\times1$ mm. Each tile was polished mechanically on both sides, etched in methanol for 10 s, to remove surface damage, and then immediately and vigorously rinsed in a jet of diethyl ether. Individual EBSD samples were then produced by cutting each tile into $4\times4\times1$ mm fragments.

2.2. In-situ SEM experiments

2.2.1. Heating and SE imaging

Samples were statically heated under vacuum ($\sim10^{-6}$ torr) to temperatures of 400–450 °C in a field-emission gun (FEG) *CamScan X500* SEM, fitted with an Oxford Instruments heating stage. The new design of the SEM satisfies the EBSD geometrical requirement of a high angle between incoming electron beam and specimen surface and maintaining the heating stage in a horizontal orientation (Seward et al., 2002). The samples were located into the heating stage by cementing them to the graphite sample holder, embedded in the graphite furnace block, using two spots of graphite paste (Fig. 1a). Calibration runs showed a temperature difference between graphite sample holder (carbon block surface) and sample upper surface of $\sim$60 °C (Fig. 1b).

In addition, test experiments were conducted (Piazolo et al., 2005b), during which a trial sample was heated to

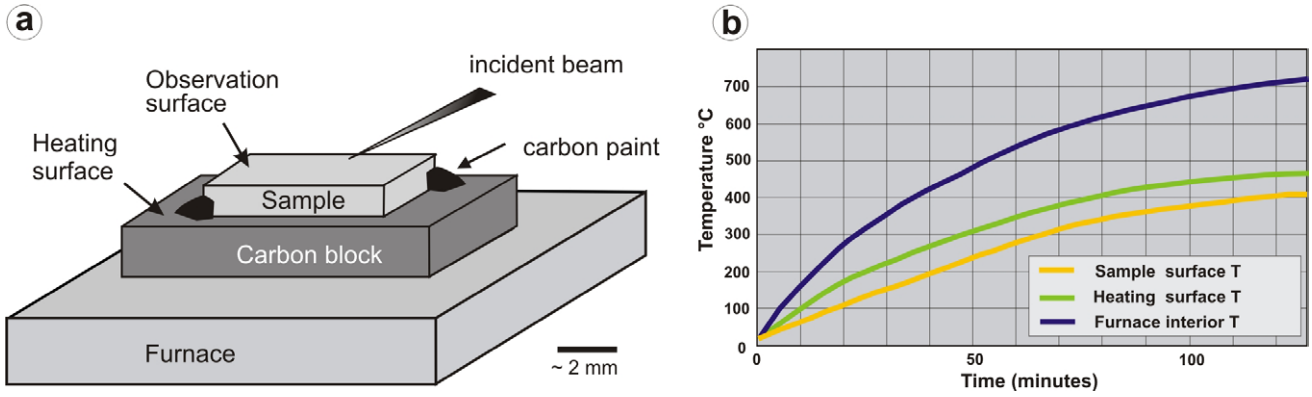

Fig. 1. (a) Sketch of experimental set-up showing the sample positioned on a carbon block that is itself sitting on top of the furnace surface. (b) Data from thermocouple measurements at sample surface, heating surface (carbon block surface) and inside the furnace.

successively higher temperatures in 20 °C steps for time intervals of 15 min duration. After each heating step, both the observation and heating surface (Fig. 1a) were mapped using EBSD. From the timing of the onset of microstructural change, the difference in temperature between the heating and observation surfaces could be shown to be <20 °C. Temperatures quoted henceforth in the text refer to the estimated temperatures at the sample observation surface. In addition to experiments with the pre-deformed rocksalt (PK98-5) we also conducted control experiments with undeformed, substructure-free NaCl samples to investigate the possible influence of radiation damage induced during EBSD analysis and strains induced by thermal expansion.

Microstructural changes were observed on the polished and etched sample surface using both secondary electron (SE) imaging and electron backscatter diffraction (EBSD) mapping technique. We found SE imaging to be more useful than orientation contrast (OC) imaging to observe microstructural development during in-situ heating of salt. Due to the sample surface preparation, it was not possible to obtain high quality OC images. In SE mode, however, grain boundaries in our samples started to 'glow' from a temperature of 200–250 °C upwards (Fig. 2), which may be the result of boundary-related trace elements and/or of an increased activation of boundary electrons.

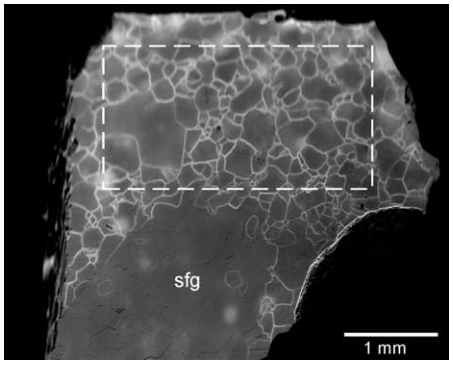

Fig. 2. Secondary electron image (SEI) at ~450 °C, using 20 kV acceleration voltage and a beam current of 7 nA. '*sfg*' marks a large strain-free grain, which already has consumed part of the old microstructure. Dashed rectangular marks ESBD map area.

Our in-situ annealing experiments were carried out in a stepwise manner. The samples were first heated from 25 to 400 °C in ~30 min and then allowed to reach ~450 °C over a further 15 min. This temperature was maintained for a specific time between 1 and 2 h. To stop any further microstructural development during orientation measurement after this elapsed time, the temperature was then dropped rapidly to 100 °C. This slightly elevated temperature ensures that no charging builds up on the sample surface to influence the orientation measurements (Seward et al., 2002). In this way, after each heating period and subsequent drop to 100 °C, the microstructure was mapped by automated EBSD analysis (e.g. Trimby et al., 2000; Humphreys, 2001). The sample documented in this paper was heated four times to ~450 °C and kept at that temperature for 2.5, 3.5, 4.5 and 6 h before cooling to 100 °C for EBSD analysis.

2.2.2. EBSD data acquisition and indexing

Full crystallographic orientation data were obtained from EBSD patterns using a 20 kV acceleration voltage and a beam current of 7 nA. EBSD patterns were auto-indexed using the CHANNEL 5.03 software of HKL Technology. The centre of 5–6 Kikuchi bands was detected automatically, whereby the solid angles calculated from the patterns were compared with the calculated halite patterns originating from 47 reflectors.

After each heating step the microstructure was mapped by multiple beam maps (6 horizontal×5 vertical). In each beam map an area of 500×400 μm was analysed with a fixed step size of 2 μm at a magnification of 240×. This step size ensured that (sub)grains <10 μm still contain several measurement points. The multiple maps are then stitched together to represent a continuous map of the whole analysed area. The average percentage of EBSD patterns that could not be indexed ranged between 10 and 15%. The maps were processed to remove erroneous data in order to provide a more complete reconstruction of the

microstructure (Prior et al., 2002). The accuracy of individual EBSD orientation measurements is better than 1°. In each individual beam map (area 500×400 μm), an orientation error <1.5° exists between points at the extremes of the scan. This is less than 2°, the smallest angle assigned to subgrain boundaries in this study (Prior, 1999; Humphreys et al., 2001). The misorientation angle was calculated by selecting the minimum misorientation angle and its corresponding axis from all possible symmetric variants (Wheeler et al., 2001). Boundaries related to different misorientation intervals are presented as coloured lines on the orientation maps.

In the orientation maps, each pixel represents an orientation, colour-coded with respect to its three Euler angles. Because of the way that Euler angles are defined, sudden changes in orientation can occur that do not correspond to large changes in orientation (see Bestmann and Prior, 2003). The orientation colours are transparently superposed onto the EBSD pattern quality parameter (Prior et al., 2002). This parameter is strongly related to surface damage and thus reproduces surface topography e.g. etched grain boundaries. The surface topography did not change significantly during heating; thus the initial grain boundary network before heating (Fig. 3, maps I) is still recognisable as a surface relict in the altered (heated) microstructure (Fig. 3, maps II–IV).

3. Results

Two different types of grain boundary migration (GBM) were observed during our static heating experiments in the SEM (Fig. 3a):

1. Slow grain boundary migration (grain boundary velocity 10^{-9}–10^{-10} m/s) between initially present substructured grains.
2. Fast GBM (grain boundary velocity 10^{-7}–10^{-6} m/s), in which new grains that are substructure-free grow at the expense of the old substructured grains. These new grains always originate from the interior (below the surface) of the specimen and can grow to large size (up to 1 mm diameter; Fig. 3a).

GBM between deformed grains is commonly observed in post-mortem microstructural studies of deformed rocks (Urai et al., 1986), but detailed knowledge about ongoing processes are lacking (see above). In this article, we will restrict attention to the slow GBM processes between substructured grains, focusing on the results obtained from a single sample of deformed salt (sample no. PK98-5). The microstructural evolution related to fast GBM is presented in the companion paper of Piazolo et al. (2005b).

Before heating, the microstructure of the deformed rocksalt sample (PK98-5; grain size range 20–400 μm) showed a high density of internal subgrain boundaries, with a misorientation angle of <15° (Fig. 3a–c). Upon static heating in the SEM, subgrain boundaries within individual grains rearranged (Figs. 3b and c and 4a), and moved (Fig. 3c). In this process, the misorientation angle of pre-existing subgrain boundaries often increased (Fig. 3b), some subgrain boundaries vanished and some new ones developed (Fig. 3b). Where slow GBM occurred, the following qualitative observations were made: (a) the growing grain developed new subgrain boundaries in the swept area (Figs. 3c and 4a); (b) the existing substructure of the growing grain propagated into the swept area (Fig. 3d); (c) individual pre-existing subgrain boundaries in the consumed grain were inherited by the growing grain (Fig. 3c); (d) at the exact location of the pre-existing high-angle grain boundary (misorientation angle >15°), a subgrain boundary (misorientation angle <15°) developed in the growing grain (Fig. 3c); and (e) substructured grains grew from the third dimension into the plane of observation (Fig. 3b).

In addition, the following observations were made regarding subgrain misorientations and subgrain density distributions. During slow GBM, the misorientation axes of rearranged subgrain boundaries, and of new subgrain boundaries are similar to the misorientation axes of subgrain boundaries prior to heat treatment (Fig. 4). The misorientation axes continue to show a girdle distribution perpendicular to the pre-heating compression direction (σ_1). Statistically, there is also little change in the density of subgrain boundaries behind migrating grain boundaries, compared with annealed material (Fig. 5). Moreover, no specific high-angle grain boundaries (misorientation angle >15°) could be identified to have significantly higher mobility than other grain boundaries. From the initial microstructure (characterised by grain size, internal subgrain structure and misorientation), preferred growth of specific grains at the expense of neighbouring grains is not expected. Note that in the control heating experiments of previously undeformed, substructure-free NaCl samples, slow grain boundary migration took place but no intracrystalline substructure development occurred behind the migrating boundaries (Fig. 6).

4. Discussion

Before attempting to interpret our detailed observations on slow grain boundary migration in the deformed samples, we first consider the crucial question of whether or not our results might be artefacts introduced by the experimental approach adopted. The ability of fast GBM, in particular, to sweep through the sample suggests that there is no significant dilatancy on existing boundaries and that neither this nor grain boundary grooving significantly impedes boundary migration. In addition, the control experiments demonstrate that the substructural features that developed behind (slowly) migrating grain boundaries during the experiments on the deformed material are unlikely to be due

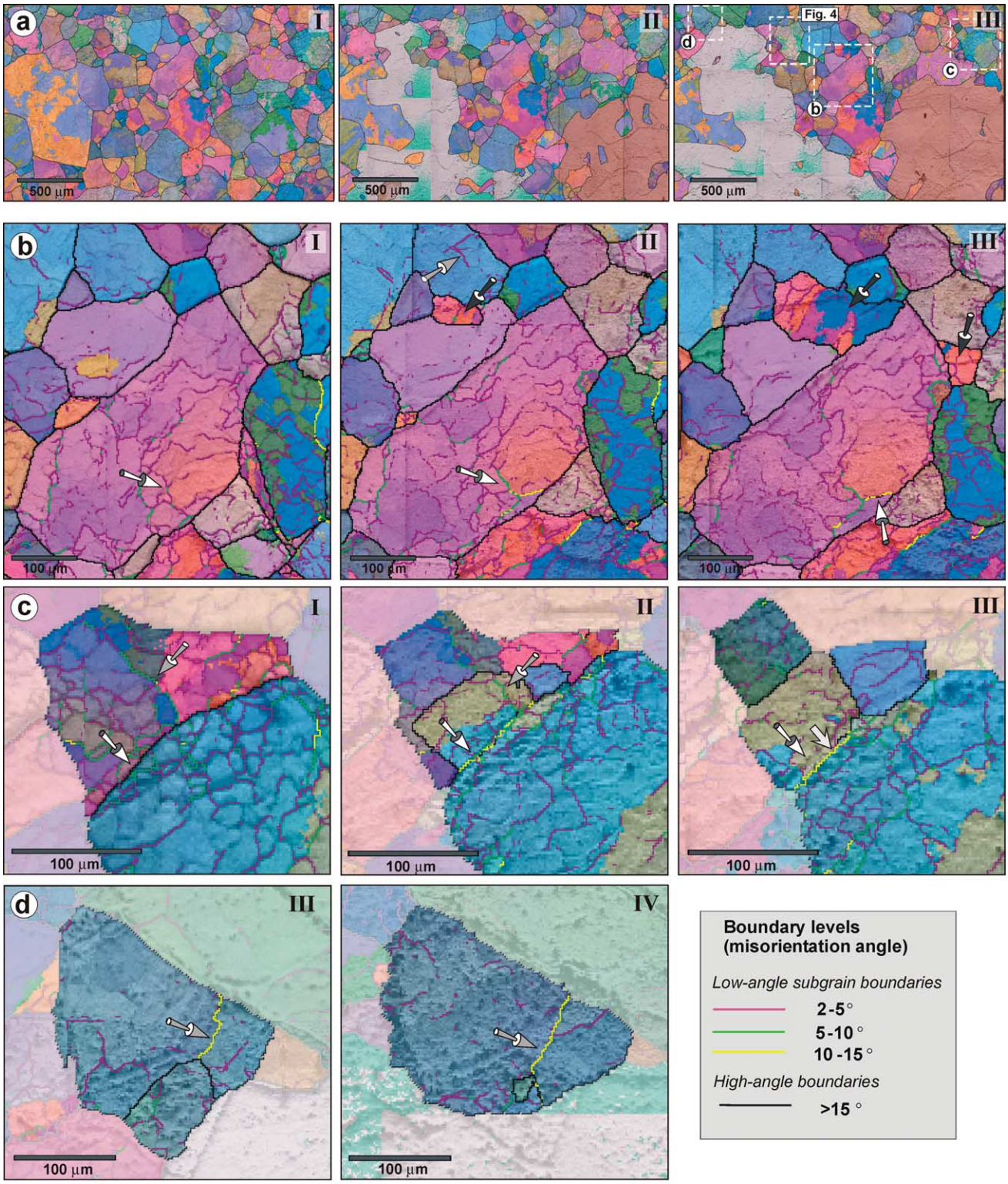

Fig. 3. Orientation maps constrained from automated EBSD analyses (sample no. PK98-5). Orientation mapping was carried out after specific static heating intervals; before heating (map I), after 2.5 h (map II), 4.5 h (map III) and 6 h heating at ~450 °C (map IV). (a) Orientation maps of total scan area. Large grey and brown areas in maps II and III represent grain growth of substructure-free grains. (b)–(d) Examples of specific microstructural features related to slow GBM during static heating (location is given in (a)). (b) Increase of misorientation angle at subgrain boundary (white arrow), development of new subgrain boundary (grey arrow) and grain growth of substructured 'old' grain from the third dimension (dark grey arrows). (c) Inheritance of pre-existing boundary structure of swept area. Grey arrow indicates the inheritance of a pre-existing low-angle boundary (green line in maps I and II), white arrow the inheritance of a pre-existing high-angle boundary during grain growth. Flat arrow in map III indicates the movement of low-angle boundary. The previous location of the moving boundary is marked by round grey arrow. Note also the rearrangement of subgrain structure. (d) Propagation of subgrain boundary (arrowed) along with migrating boundary. Arrow spots on focussed subgrain boundary. Data are on a grid of 2 µm spacing. Each pixel represents an orientation, colour coded with respect to its Euler angles.

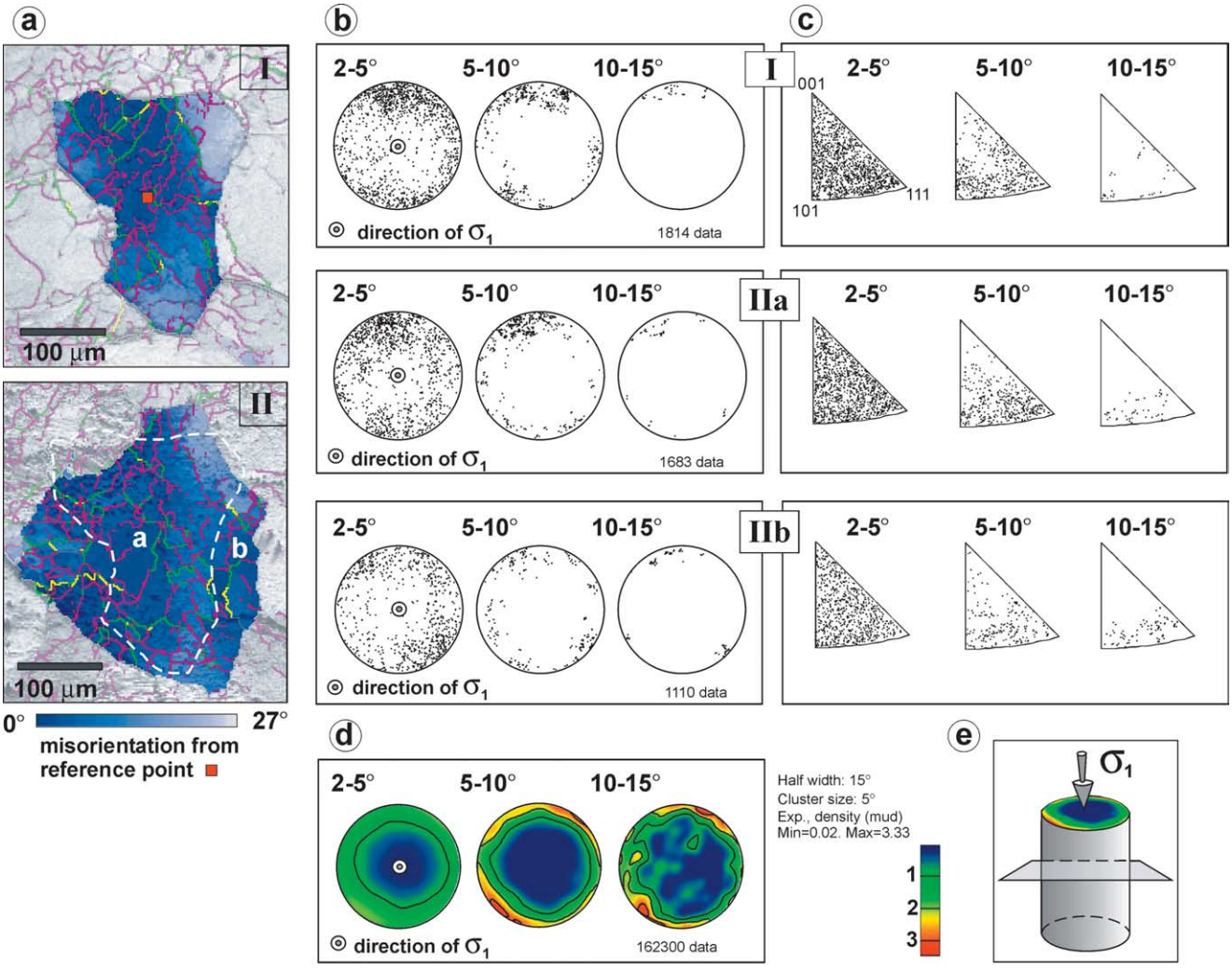

Fig. 4. Evolution of misorientation axis distribution of subgrain boundaries during static heating. (a) Rearrangement and development of subgrain boundaries during grain growth within highlighted grain. (I) Substructure of grain before and (II) after 6 h heating. (IIa) Same area as in (I), marked by white dashed line; (IIb) new substructured area of the grown grain. Substructure is colour coded according to angular misorientation from a given reference point (red square). Subgrain boundaries are colour coded as in Fig. 3. (b) and (c) Distribution of misorientation axes of subgrain boundaries for the specific areas given in (a). Misorientation axis distribution related to the sample reference frame (shown in (b) as pole figures) and with respect to the crystal system (shown in (c) as inverse pole figures; crystallographic indices are given). Data are separated into different misorientation angle intervals and are presented as equal area upper hemisphere plots. (d) Bulk distribution of misorientation axes of intracrystalline subgrain boundaries from the deformed rocksalt sample before static heating (Fig. 3a-I). (e) Orientation of the pole figures with respect to the kinematic setting of axial compression during the previous deformation of the sample. Main compression axis σ_1 is given as a symbol in the respective pole figures in (b) and (d).

to defects induced by electron beam damage (Urai et al., 1987; Donker and Garcia Celma, 1996), thermal expansion (Donker and Garcia Celma, 1996), or growth accidents during GBM (Gleiter et al., 1980; Donker and Garcia Celma, 1996). These findings are supported by calculations that show that the force due to thermal expansion is not significant in comparison with the driving forces due to defect-stored energy differences. In addition, if there were any microstructural changes due to experimental artefacts, these then would not be expected to produce substructures with a similar orientation distribution of misorientation axes as observed in the original, non-heated, deformed sample (see below).

We now focus on the differences between the slow and fast GBM behaviours seen in our deformed samples. Migration of grain boundaries between grains in plastically deformed materials is generally regarded as being driven mainly by spatial (grain-to-grain) differences in the stored strain energy carried by dislocation (Bell and Etheridge, 1976; White, 1976). Since the difference in free dislocation density across boundaries between substructured old grains and substructure-free new grains is much bigger than between substructured old grains, the driving force and hence the GBM velocity is expected to be significantly higher. Depending on the time–temperature path, the microstructure may end up with the near-complete consumption of substructured grains by the fast growth of new strain-free grains (see also Ree and Park, 1997; Nam et al.,

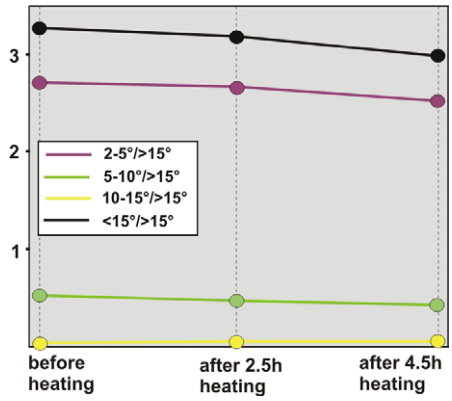

Fig. 5. Evolution of subgrain boundary (<15°) density during heating experiments. The total length of subgrain boundaries with different misorientation angle intervals (see key) was related to the total length of high angle boundaries (>15°). The area covered by large strain-free grains was excluded for the analysis.

1999). However in most experiments, even after long static heating, relicts of substructured grains were still evident (for detailed description see Piazolo et al. (2005b)).

The conventional model of strain-induced GBM (Hillert, 1965; Drury et al., 1985; Urai et al., 1986) predicts that the less strained grain grows at the expense of the more strained grain and that dislocations are absorbed by the moving boundary. In the static case, the strain induced grain boundary bulging into grain 2 (Fig. 7b) leaves a strain-free region (low dislocation density) behind the migrating boundary and is substructure-free or substructure poor (Bailey and Hirsch, 1962; Bell and Etheridge, 1976; White, 1976; Urai, 1987; Humphreys and Hatherly, 1995).

In our static annealing experiments on deformed salt, the propagation of subgrain boundaries from old to new grain portions during GBM can be argued to be consistent with this conventional model, with excess dislocations in the consumed material being removed by and driving GBM (Fig. 7c). This propagation process, referred to as edgewise propagation of subgrain boundaries by Means and Dong (1982), is consistent with numerical models of strain induced GBM (Humphreys and Hatherly, 1995), TEM analysis of deformed copper (Bailey and Hirsch, 1962) and rock analogue experiments (Means, 1983; Means and Ree, 1988; Park et al., 2001).

In contrast, the development of entirely new subgrain boundaries behind migrating grain boundaries appears inconsistent with the conventional model for strain-induced GBM. It is possible that these new subgrain boundaries have propagated from the third dimension and it is impossible to rule out that the effect of the free surface has been to drive a shift in the balance of substructures between the sample interior and the free surface. Perhaps the best argument that this has not occurred is that there is no systematic change in subgrain density in areas that were not swept by new boundaries; free surface effects would be expected to affect all grains. The distribution of misorientation axes of the new subgrain boundaries is similar to that of the old subgrain boundaries (Fig. 4). This suggests that the character of the new subgrain boundaries must be linked to the dislocation structures developed during the pre-heating deformation history. During deformation, specific line defects (dislocation) were produced with a specific glide plane and glide direction related to the external stress field (e.g. Hull and Bacon, 1984). During recovery dislocations progressively move through the lattice and pile up in subgrain boundaries, which can be characterised by their misorientation axes. Such dislocation structures and thus the distribution of misorientation axes are related to the magnitude and symmetry of the externally applied differential stress field and the resultant accommodated strain (Kocks, 1976; Bestmann and Prior, 2003). Since no new dislocation structures were induced during static heating (Fig. 6) pre-existing free and wall-bound dislocations present in the old material behind a migrating grain boundary might therefore move into the newly swept areas and rearrange themselves to form new substructures. Thus the processes active during resumption of recovery (recovery also occurred during deformation) are still controlled by the previous

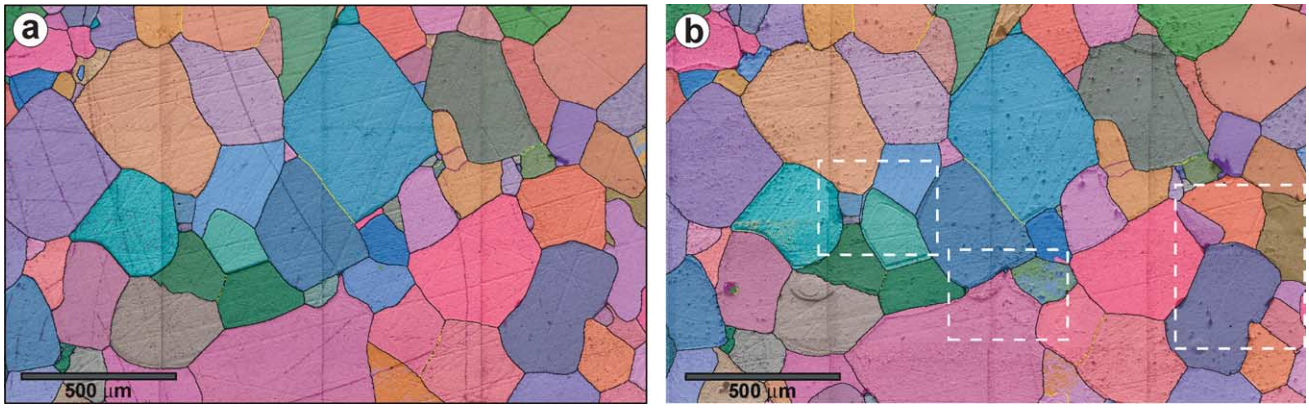

Fig. 6. Processed EBSD orientation maps of exemplary control experiments using an undeformed rocksalt sample (sample no. PK84). (a) Microstructure before heating and (b) after 1 h heating at 450–500 °C. Dashed lined rectangles show areas where grain boundary migration has occurred. Note that no new substructures are developed. Data are on a grid of 2 µm spacing. For boundary levels see Fig. 3.

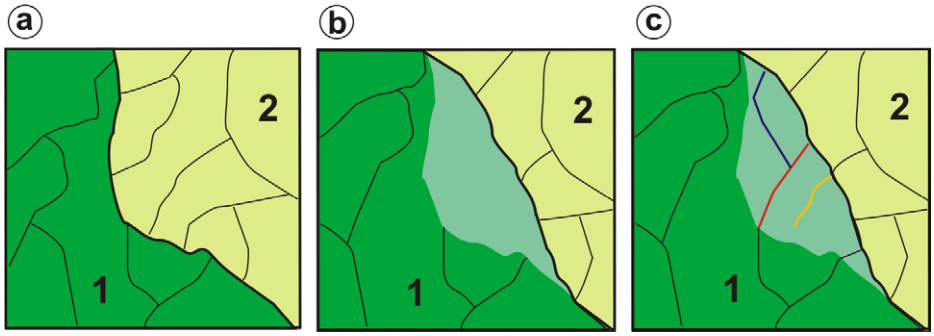

Fig. 7. Diagrams show schematically the microstructural development of an initial microstructure (a) during grain boundary migration (GBM). During GBM grain 1 sweeps over an area formerly occupied by grain 2. (b) Traditionally, the swept area is thought to be dislocation and therefore subgrain boundary free (Hillert, 1965; Urai et al., 1986). (c) According to our experimental results subgrain boundaries develop in the swept area. These new subgrain boundaries are either completely new (dashed), or continue subgrain boundaries of the sweeping grain (dash–dotted), or show similar locations and angular relationships as the swept grain (dotted).

deformation event and results in the same character of substructures reflected by the characteristic distribution of misorientation axes. Nevertheless, although these new subgrain structures develop, the total length of low-angle boundaries decreases during the heating experiments (Fig. 5). This points to an overall, slight but significant drop in stored energy of the system which is, on thermodynamic considerations, expected.

Finally, the observed inheritance of relict substructures from the consumed grain suggests that lattice dislocations were incorporated from the crystal ahead of the migrating boundary. This could possibly be explained by a collective jump of atoms across a migrating grain boundary (Merkle et al., 2002), provided that the inherited dislocation structure has a lower energy than that of the consumed material. This contrasts sharply, however, with the conventional model in which atoms diffuse one by one across a boundary, driven by differences in subgrain stored energy (e.g. Derby, 1990).

5. Geological implications

The frozen-in microstructure after static heating closely resembles that before heating and both are very similar to the results of other salt deformation experiments (Guillopé and Poirier, 1979b; Franssen, 1994) and to the microstructures of naturally deformed rocks (e.g. Urai et al., 1987). A number of important implications can be inferred for tectonites that have undergone late, static recrystallization dominated by the slow strain energy induced GBM process.

Firstly, misorientation axis distributions may provide a relatively robust indicator of deformation mechanisms and conditions, and subgrain sizes may increase slightly but generally show the same order of magnitude as the deformation-induced pre-anneal microstructure. Secondly, models for the effect of GBM in both static and dynamic recrystallization may need to be modified, because the driving force for GBM is often assumed to be due primarily to complete dissipation of subgrain stored energy (Guillopé and Poirier, 1979a; Shimizu, 1998). Thirdly, when interpreting microstructures in nature the geologist needs to be cautious when assuming that the presence of subgrain structure in a deformed material rules out static recrystallization by GBM. Some apparently dynamically recrystallized microstructures may actually have undergone significant static recrystallization, with substructures like those observed in our experiments.

However, many examples exist in nature and experiments (e.g. Heilbronner and Tullis, 2002; Park et al., 2001; Barnhoorn, 2003), where after annealing no substructures are preserved. If we consider substructure migration and reorganisation of free dislocations into subgrain boundaries during annealing as an important process, the lack or occurrence of intracrystalline deformation structures in experimental or natural samples seems also to depend on absolute temperatures and timing of the temperature evolution during annealing after deformation has stopped. Especially the preservation potential of substructures in deformed-then-annealed rocks depends on the occurrence and significance of fast GBM. For dominant fast GBM the level of initial internal strain energy must be high enough to allow the nucleation of new strain-free grains (e.g. Doherty et al., 1997). A recent study of Piazolo et al. (2005), for example, showed that similar features to those observed in our experiments, are also seen in naturally heated quartz grains from a thermal aureole. They can show a continuation of substructures and twin boundaries as well as the development of new low-angle substructures and twin boundaries during grain boundary migration.

It is important to recall that the salt samples investigated in this study were extremely dry (<5 ppm water), as a result of both pre-deformation drying and in-situ heating in the high vacuum environment of the SEM. However, a few tens of ppm's of water are known to have a strong influence on microstructural change in salt (and other) rocks, dramatically accelerating grain boundary migration via fluid-assisted interfacial transfer (see Urai, 1985, 1987; Urai et al., 1986; Spiers et al., 1988; Drury and Urai, 1990; Peach et

al., 2001; Watanabe and Peach, 2002; Ter Heege et al., 2004, 2005). Since natural rocksalt is invariably wet (i.e. contains $>>$50–100 ppm water: Roedder, 1984; Carter et al., 1993; Spiers and Carter, 1998), the results of our 'dry' rocksalt experiments should be applied only with caution to natural rocksalt, or indeed to other rocks showing fluid-assisted grain boundary migration. Rather, we view our present data as indicative of previously unreported phenomena that can occur during static recrystallization of rocks and minerals and which have a potentially important bearing on interpreting natural and experimental microstructures. Clearly, further detailed work is needed to assess the importance of the presented microstructural features in a variety of tectothermal settings.

6. Conclusions

In-situ heating experiments investigating static recrystallization and recovery phenomena in rocksalt using EBSD analysis yield the following main findings:

(1) Static heating of a previously deformed crystalline material can result in a microstructure that is similar to a frozen-in deformed microstructure.
(2) Subgrain characteristics such as rotation axes are robust indicators of the type of deformation even if significant grain boundary migration took place during static heating.
(3) Simple, single-atom jump models of grain boundary migration do not explain all observed features.
(4) Interpretations of microstructure should take into account these findings, especially when used to place constraints on the deformation/recrystallization history.

Acknowledgements

We thank Peter van Krieken for preparing the samples and Gareth Seward for an introduction to conducting in-situ heating experiments. The manuscript benefited significantly from constructive reviews by Marco Herwegh and Janos Urai. Bernhard Grasemann and Mark Handy are acknowledged for their comments on the manuscript. Michel Bestmann and Sandra Piazolo kindly acknowledge financial support by DFG-grant BE 2413/1-1 and Marie Curie Fellowship HPMF-CT-2001-01457, respectively. The *CamScan X500* was funded by HEFCE through the grant JR98LIPR. These experiments were funded by NERC grant NER/A/5/2001/01181. The final revision of the manuscript was done and funded by FWF project 15668 in Vienna, Austria.

References

Bailey, J.E., Hirsch, P.B., 1962. The recrystallization process in polycrystalline metals. Proceedings of Royal Society of London A267, 11–30.

Barnhoorn, A., 2003. Rheology and microstructural evolution of carbonate rocks during large strain torsion experiments. Dissertation, ETH, Zürich, Nr. 15309.

Beck, P.A., 1949. Comments on grain growth in octachloropropane. Journal of Applied Physics 20, 231.

Bell, T., Etheridge, M.A., 1976. The deformation and recrystallization of quartz in a mylonite zone, Central Australia. Tectonophysics 32, 238–267.

Bestmann, M., Prior, D.J., 2003. Intragranular dynamic recrystallization in naturally deformed calcite marble: diffusion accommodated grain boundary sliding as a result of subgrain rotation recrystallization. Journal of Structural Geology 25, 1597–1613.

Bons, P.D., Urai, J.L., 1992. Syndeformational grain growth: microstructures and kinetics. Journal of Structural Geology 14, 1101–1109.

Burg, J.P., Wilson, C.J.L., Mitchell, J.C., 1986. Dynamic recrystallization and fabric development during the simple shear deformation of ice. Journal of Structural Geology 8, 857–870.

Carter, N.J., Horseman, S.T., Russell, J.E., Handin, J., 1993. Rheology of rocksalt. Journal of Structural Geology 15, 1257–1271.

Derby, B., 1990. Dynamic recrystallization and grain size, in: Barber, D.J., Meredith, P.G. (Eds.), Deformation Processes in Minerals Ceramics and Rocks The Mineralogical Society Series, 1. Unwin Hyman, London, pp. 354–362.

Doherty, R.D., Hughes, D.A., Humphreys, F.J., Jonas, J.J., Jensen, D.J., Kassner, M.E., King, W.E., McNelley, T.R., McQueen, H.J., Rollett, A.D., 1997. Current issues in recrystallization: a review. Material Science and Engineering A 238, 219–274.

Donker, H., Garcia Celma, A., 1996. Saturation of radiation damage in natural rock salt irradiated at moderate dose rate. Radiation Effects and Defects in Solids 139, 241–252.

Drury, M.R., Urai, J.L., 1990. Deformation-related recrystallization processes. Tectonophysics 172, 235–253.

Drury, M.R., Humphreys, F.J., White, S.H., 1985. Large strain deformation studies using polycrystalline magnesium as a rock analogue. Part II: dynamic recrystallisation mechanisms at high temperatures. Physics of the Earth and Planetary Interiors 40, 208–222.

Duval, B., Cramez, C., Jackson, M.P.A., 1992. Raft tectonics in the Kwanza basin, Angola. Marine and Petroleum Geology 9, 389–404.

Franssen, R.C.M.W., 1994. The rheology of synthetic rocksalt in uniaxial compression. Tectonophysics 233, 1–40.

Gemperlova, J., Jacques, A., Gemperle, A., Vystavel, T., Zarubova, N., Janecek, M., 2002. In-situ transmission electron microscopy observation of slip propagation in 3 bicrystals. Materials Science and Engineering Series A 324, 183–189.

Gleiter, H., Mahajan, S., Bachmann, K.J., 1980. The generation of lattice dislocations by migrating boundaries. Acta Metallurgica 28, 1603–1610.

Guillopé, M., Poirier, J.-P., 1979a. Deformation induced recrystallization of minerals. Bulletin Minéral 102, 67–74.

Guillopé, M., Poirier, J.-P., 1979b. Dynamic recrystallization during creep of single-crystalline halite: an experimental study. Journal of Geophysical Research 84, 5557–5567.

Heilbronner, R., Tullis, J., 2002. The effect of static annealing on microstructures and crystallographic preferred orientations of quartzites experimentally deformed in axial compression and shear, in: de Meer, S., Drury, M.R., de Bresser, J.H.P., Penncock, G.M. (Eds.), Deformation Mechanisms, Rheology and Tectonics: Current Status and Future Perspectives Geological Society, London, Special Publications, 200, pp. 191–218.

Herwegh, M., Handy, M.R., 1996. The evolution of high-temperature mylonitic microfabrics: evidence from simple shearing of a quartz analogue (norcamphor). Journal of Structural Geology 18, 689–710.

Hillert, M., 1965. On the theory of normal and abnormal grain growth. Acta Metallurgica 13, 227–238.

Hobbs, B.E., 1985. The geological significance of microfabric, in: Wenk, H.R. (Ed.), Preferred Orientation in Deformed Metals and Rocks: An Introduction to Modern Texture Analysis. Academic Press, New York, pp. 463–484.

Hull, D., Bacon, D.J., 1984. Introduction to Dislocations. Pergamon Press, Oxford. 242pp.

Humphreys, F.J., 1979. The nucleation of recrystallization at second phase particles in deformed aluminium. Acta Metallurgica 25, 1323–1344.

Humphreys, F.J., 2001. Review—grain and subgrain characterisation by electron backscatter diffraction. Journal of Materials Science 36, 3833–3854.

Humphreys, F.J., Hatherly, M., 1995. Recrystallization and Related Annealing Phenomena. Pergamon Press, Oxford. 498pp.

Humphreys, F.J., Ferry, M., Johnson, C.P., Brough, I., 1996. Combined in situ annealing and EBSD of deformed alloys. Textures and Microstructures 281, 26–27.

Humphreys, F.J., Bate, P.S., Hurley, P.J., 2001. Orientation averaging of EBSD data. Journal of Microscopy 201, 50–58.

Jackson, M.P.A., 1995. Retrospective salt tectonics, in: Jackson, M.P.A., Roberts, D.G., Snelson, S. (Eds.), Salt Tectonics: a Global Perspective AAPG Memoir, 65, pp. 1–28.

Jessell, M.W., 1986. Grain boundary migration and fabric development in experimentally deformed octachloropropane. Journal of Structural Geology 8, 527–542.

Kocks, U.F., 1976. Laws for work-hardening and low-temperature creep. Journal Engineering, Materials and Technology 98, 76–85.

Le Gall, R., Liao, G., Saindrenan, G., 1999. In situ SEM studies of grain boundary migration during recrystallization of cold-rolled nickel. Scripta Materialia 41, 427–432.

Means, W.D., 1983. Microstructure and micromotion in recrystallization flow of octachloropropane: a first look. Geologische Rundschau 72, 511–528.

Means, W.D., Dong, H., 1982. Some unexpected effects of recrystallization on the microstructures of material deformed at high temperatures. Mitteilungen des Geologischen Instituts ETH, Neue Folge 239a.

Means, W.D., Ree, J.H., 1988. Seven types of subgrain boundaries in octachloropropane. Journal of Structural Geology 10, 765–770.

Means, W.D., Xia, Z.G., 1981. Deformation of crystalline materials in thin section. Geology 9, 538–543.

Merkle, K.L., Thompson, L.J., Phillipp, F., 2002. Collective effects in grain boundary migration. Physical Review Letters 88, 2,255,011–2,255,014.

Nam, T.N., Otoh, S., Masuda, T., 1999. In-situ annealing experiments of octachloropropane as a rock analogue: kinetics and energetics of grain growth. Tectonophysics 304, 57–70.

Park, Y., Ree, J.-H., Kim, S., 2001. Lattice preferred orientation in deformed-then-annealed material: observations from experimental and natural polycrystalline aggregates. International Journal of Earth Sciences (Geologische Rundschau) 90, 127–135.

Peach, C.J., Spiers, C.J., 1996. Influence of plastic deformation on dilatancy and permeability development in synthetic salt rock. Tectonophysics 256, 101–128.

Peach, C.J., Spiers, C.J., Trimby, P.W., 2001. Effect of confining pressure on latation, recrystallization and flow of rocksalt at 150 °C. Journal of Geophysical Research 106, 13,315–13,328.

Piazolo, S., Prior, D.J., Holness, M.D., 2005a. The use of combined Cathodoluminescence and EBSD analysis: a case study investigating the grain growth mechanisms in quartz. Journal of Microscopy, in press.

Piazolo, S., Bestmann, M., Spiers, C., Prior, D.J., 2005b. Temperature dependent grain boundary migration in deformed-then-annealed material: observations from experimental polycrystalline rock salt.

Prior, D.J., 1999. Problems in determining the misorientation axes, for small angular misorientations, using electron backscatter diffraction in the SEM. Journal of Microscopy 195, 217–225.

Prior, J.D., Wheeler, J., Peruzzo, L., Spiess, R., Storey, C., 2002. Some garnet microstructures: an illustration of the potential of orientation maps and misorientation analysis in microstructural studies. Journal of Structural Geology 24, 999–1011.

Ree, J.H., 1990. High temperature deformation of octachloropropane: dynamic grain growth and lattice reorientation, in: Knipe, R.J., Rutter, E.H. (Eds.), Deformation Mechanisms, Rheology and Tectonics Special Publications of the Geological Society of London, 54, pp. 363–368.

Ree, J.H., Park, Y., 1997. Static recovery and recrystallization microstructures in sheared octachloropropane. Journal of Structural Geology 19, 1521–1526.

Roedder, E., 1984. The fluids in salt. American Mineralogist 69, 413–439.

Schmid, S., 1982. Microfabric studies as indicators of deformation mechanisms and flow laws operative in mountain building, in: Hsu, K.J. (Ed.), Mountain Building Processes. Academic Press, London, pp. 95–110.

Seward, G.G.E., Prior, D.J., Wheeler, J., Celotto, S., Halliday, D.J.M., Paden, R.S., Tye, M.R., 2002. High-temperature electron backscatter diffraction and scanning electron microscopy imaging techniques: in-situ investigations of dynamic processes. Scanning 24, 232–240.

Seward, G.G.E., Celotto, S., Prior, D.J., Wheeler, J., Pond, R.C., 2004. In situ SEM–EBSD observations of the hcp to bcc phase transformation in commercially pure titanium. Acta Materialia 52, 821–832.

Shimizu, I., 1998. Stress and temperature dependence of recrystallized grain size: a subgrain misorientation model. Geophysical Research Letters 25, 4,237–4,240.

Spiers, C.J., Carter, N.L., 1998. Microphysics of rocksalt flow in nature, in: Aubertin, M. (Ed.), The Mechanical Behaviour of Salt: Proceedings of the Fourth Conference Trans Tech Publication Series on Rock and Soil Mechanics, 22, pp. 115–128.

Spiers, C.J., Urai, J.L., Lister, G.S., 1988. The effect of brine (inherent or added) on the rheology and deformation mechanisms in salt rock, in: Hardy Jr., H.R., Langer, M. (Eds.), The Mechanical Behaviour of Salt: Proceedings of the Second Conference Series on Rock and Soil Mechanics, Trans Tech Publications, pp. 89–102.

Ter Heege, J.H., de Bresser, J.H.P., Spiers, C.J., 2004. Dynamic recrystallization of dense polycrystalline NaCl: dependence of grain size on stress and temperature. Materials Science Forum 467–470, 1187–1192.

Ter Heege, J.H., de Bresser, J.H.P., Spiers, C.J., 2005. Dynamic recrystallization of wet synthetic polycrystalline halite: dependence of grain size distribution on flow stress, temperature and strain. Tectonophysics, in press.

Trimby, P.W., Drury, M.R., Spiers, C.J., 2000. Misorientation across etched boundaries in deformed rocksalt: a study using electron backscatter diffraction. Journal of Structural Geology 22, 81–89.

Tungatt, P.D., Humphreys, F.J., 1981. An in-situ optical investigation of the deformation behaviour of sodium nitrate—an analogue for calcite. Tectonophysics 78, 661–675.

Urai, J.L., 1985. Water-enhanced dynamic recrystallization and solution transfer in experimentally deformed carnallite. Tectonophysics 120, 285–317.

Urai, J.L., 1987. Development of microstructure during deformation of carnallite and bischofite in transmitted light. Tectonophysics 135, 251–263.

Urai, J.L., Humphreys, F.J., 1981. The development of shear zones in polycrystalline camphor. Tectonophysics 78, 677–685.

Urai, J.L., Jessell, M., 2001. Recrystallization and grain growth in minerals: recent developments, in: Gottstein, G., Molodov, D. (Eds.), Recrystallization and Grain Growth Proceedings of the First Joint International Conference, RWTH Aachen, Germany. Springer Verlag, Berlin, pp. 87–96.

Urai, J.L., Humphreys, F.J., Burrows, S.E., 1980. In-situ studies of the deformation and dynamic recrystallisation of rhombohedral camphor. Journal of Material Sciences 15, 1231–1240.

Urai, J.L., Means, W.D., Lister, G.S., 1986. Dynamic recrystallization of

minerals, in: Hobbs, B.E., Heard, H.C. (Eds.), Mineral and Rock Deformation: Laboratory Studies (the Paterson Volume) Geophysical Monograph of American Geophysical Union, 36, pp. 161–200.

Urai, J.L., Spiers, C.J., Peach, C.J., Franssen, R.C.M.W., Liezenberg, J.L., 1987. Deformation mechanisms operating in naturally deformed halite rocks as deduced from microstructural investigations. Geologie en Mijnbouw 66, 164–176.

Watanabe, T., Peach, C.J., 2002. Electrical impedance measurement of plastically deforming halite rocks at 125 °C and 50 MPa. Journal of Geophysical Research, B, Solid Earth and Planets 107, 1–12.

Wheeler, J., Prior, D.J., Jiang, Z., Spiess, R., Trimby, P.J., 2001. The petrological significance of misorientations between grains. Contributions to Mineralogy and Petrology 141, 109–124.

White, S., 1976. The effects of strain on the microstructures, fabrics, and deformation mechanisms in quartzites. Royal Society of London Philosophical Transactions Series A 283, 69–86.

White, S., 1977. Geological significance of recovery and recrystallization processes in quartz. Tectonophysics 39, 143–170.

Wilson, C.J.L., 1985. In-situ recrystallization of ice. Journal of Structural Geology 7, 500.

Zhang, Y., Wilson, C.J.L., 1997. Lattice rotation in polycrystalline aggregates and single crystals with one slip system: a numerical and experimental approach. Journal of Structural Geology 19, 875–885.